

1 Contents

2 3 Investigation of solar irradiance variations and their impact on	
3 middle atmospheric ozone	1
4 M. Weber, J. Pagaran, S. Dikty, C. von Savigny, J. P. Burrows,	
5 M. DeLand, L. E. Floyd, J. W. Harder, M. G. Mlynczak, H. Schmidt	
6 3.1 Introduction	2
7 3.2 SCIAMACHY spectral solar irradiance	4
8 3.3 Irradiance variations from solar rotations to several solar cycles	6
9 3.4 Solar rotation (27-day) signature in stratospheric ozone	8
10 3.5 Daytime variations in mesospheric ozone	10
11 3.6 Conclusion	12
12 References	13
13 References	18

¹⁴ **Chapter 3**

¹⁵ **Investigation of solar irradiance variations and**

¹⁶ **their impact on middle atmospheric ozone**

¹⁷ M. Weber, J. Pagaran, S. Dikty, C. von Savigny, J. P. Burrows, M. DeLand, L. E.
¹⁸ Floyd, J. W. Harder, M. G. Mlynczak, H. Schmidt

¹⁹ **Abstract** The satellite spectrometer SCIAMACHY aboard ENVISAT is a unique instrument
²⁰ that covers at a moderately high spectral resolution the entire optical range from the near UV (230 nm) to the near IR ($2.4\mu\text{m}$) with some gaps above $1.7\mu\text{m}$.
²¹ This broad spectral range allows not only the retrieval of several atmospheric trace gases (among them ozone), cloud and aerosol parameters, but also regular daily measurements of the spectral solar irradiance (SSI) with an unprecedented spectral coverage. The following studies were carried out with irradiance and ozone data from SCIAMACHY: a) SCIAMACHY SSI was compared to other solar data from space and ground as well as with SIM/SORCE (Solar Irradiance Monitor, the only other satellite instrument daily measuring the visible and near IR, in order to verify the quality of the SCIAMACHY measurements, b) an empirical solar proxy model, in short the SCIA proxy model, was developed that permits expressing the SCIA-

Mark Weber, Joseph Pagaran, Sebastian Dikty, Christian von Savigny, and John P. Burrows
Institute of Environmental Physics, University of Bremen FB1, PO Box 330 440, D-28334
Bremen, Germany e-mail: weber@uni-bremen.de

Matt T. DeLand
Science System and Applications, Inc (SSAI), 10210 Greenbelt Road, Suite 600, Lanham, MD
20706 e-mail: matthew.deland@ssaihq.com

Jerry W. Harder,
Laboratory for Atmospheric and Space Physics (LASP), University of Colorado, 1234 Innovation Drive, Boulder, CO 80303, USA e-mail: jerry.harder@lasp.colorado.edu

Linton E. Floyd
Interferometrics Inc., 13454 Sunrise Valley Drive, Herndon, Virginia, VA 20171, USA e-mail:
linton4@gmail.com

Martin G. Mlynczak
NASA Langley Research Center, Hampton, VA 23681-2199, USA e-mail:
m.g.mlynczak@nasa.gov

Hauke Schmidt
Max-Planck-Institute for Meteorology, Bundesstr. 53, 20146 Hamburg, Germany e-mail:
hauke.schmidt@zmaw.de

31 MACHY SSI variations by fitting solar proxies for faculae brightening and sunspot
 32 darkening, which then allows investigation of solar variability on time scales be-
 33 yond the instrument life time, e.g. 11-year solar cycle, c) solar cycle SSI variations
 34 derived from empirical models (Lean2000, SATIRE, SCIA proxy) and different ob-
 35 servations (SBUV composite, SUSIM) were compared for the three most recent
 36 solar cycles 21-23, and d) SCIAMACHY ozone limb profiles were analysed to de-
 37 rive signatures of the 27-day solar rotation on stratospheric ozone. Our studies were
 38 complemented by investigations of daytime variations in mesospheric ozone (here
 39 data from SABER/TIMED), which were compared to results from the HAMMO-
 40 NIA chemistry climate model.

41 3.1 Introduction

42 Regular daily space-borne satellite SSI monitoring started in 1978. The wavelength
 43 coverage of early SSI measurements from different satellite instruments was gen-
 44 erally limited to below 400 nm (UV), where the largest variations occur over an
 45 11-year solar cycle (*Rottman et al.*, 2004). A limiting factor for many space spec-
 46 trometers measuring in the UV is the optical degradation due to hard radiation that
 47 makes it challenging to maintain the accuracy over the instrument lifetime which
 48 rarely extends to more than a decade (*DeLand et al.*, 2004). In order to derive esti-
 49 mates for SSI variations over an entire 11-year solar cycle or more one needs to rely
 50 on a SSI timeseries composed of different instruments (UV composite) as done for
 51 the UV spectral range (*DeLand and Cebula*, 2008) or use solar proxies, like the Mg
 52 II index, that are well correlated with irradiance changes over a large spectral range
 53 to extrapolate beyond the instrumental lifetime (*DeLand and Cebula*, 1993; *Viereck*
 54 *et al.*, 2001).

55 Daily observations of the visible and near-IR started with the three channel SPM
 56 (Sun Photometer) of VIRGO/SOHO (1996-2010) at selected wavelength bands
 57 (*Fröhlich et al.*, 1997) and were continued with GOME/ERS-2 (Global Ozone
 58 Monitoring Experiment) since 1995, covering 240–800 nm (*Weber et al.*, 1998;
 59 *Burrows et al.*, 1999), SCIAMACHY/ENVISAT (Scanning Imaging Absorption
 60 Spectrometer for Atmospheric Chartography) since 2002, covering 220nm - 2.4 μ m
 61 (*Bovensmann et al.*, 1999), and SIM/SORCE (Solar Irradiance Monitor) since 2003,
 62 240nm–3 μ m (*Harder et al.*, 2005a,b). In Fig. 3.1 a sample SCIAMACHY solar ir-
 63 radiance spectrum is shown. Compared to the UV region, daily irradiance measure-
 64 ments simultaneously covering the UV, visible, and the near IR do not cover yet a
 65 complete solar cycle. One of the important scientific question is what are the irra-
 66 diance changes in the visible and near IR during 27-day solar rotations and can we
 67 use this information to extrapolate to changes during the 11-year solar cycle.

68 SCIAMACHY is primarily an atmospheric sounder measuring several trace
 69 gases in nadir (column amounts) and limb viewing geometry (vertical profiles)
 70 (*Bovensmann et al.*, 2011). Global vertical profiles are measured by SCIAMACHY
 71 and cover the altitude range from the tropopause to about 70 km altitude (*von Savi-*

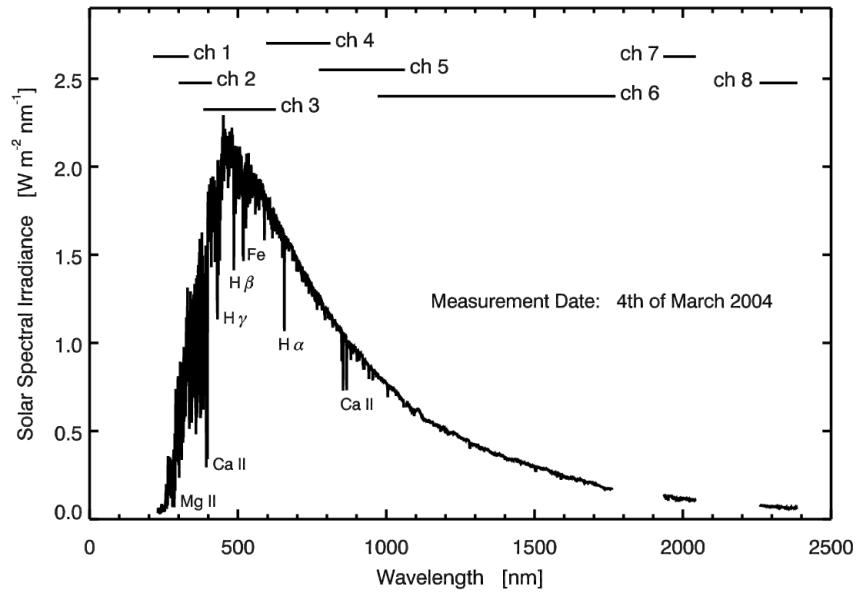


Fig. 3.1 SCIAMACHY full disc solar spectrum measured on March 4, 2004. The eight spectral channels varying in spectral resolution from 0.2 nm to 1.5 nm are indicated. The gaps near 1850 nm as well as 2200 nm are not measured by SCIAMACHY since terrestrial water vapor absorption saturates in the atmospheric observation mode. From *Pagaran et al.* (2009). Reproduced by permission of the AAS.

gny *et al.*, 2005; Sonkaew *et al.*, 2009). The influence of irradiance variations related to the 27-day mean solar rotation period on upper stratosphere ozone can be investigated using SCIAMACHY ozone data. The upper stratosphere above 30 km is chemically controlled and an immediate radiative influence on the photochemistry is expected (e.g. Gruzdev *et al.*, 2009; Fioletov, 2009). In this study for the first time a wavelet analysis was applied to study the 27-day signature in ozone. This permits the investigation of the time-varying frequency content of the ozone signal.

The non-polar orbit of the TIMED satellite (Thermosphere, Ionosphere, Mesosphere, Energetics and Dynamics) carrying the SABER instrument (Sounding of the Atmosphere using Broadband Emission Radiometry) (*Russell III et al.*, 1999) permits the study of daytime variations in mesospheric ozone that are significantly larger than the 27-day and solar cycle related changes observed in the upper stratosphere (*Huang et al.*, 2008). In this study the daytime variation of mesospheric ozone were compared for the first time with the output of a chemistry climate model (*Dikty et al.*, 2010a).

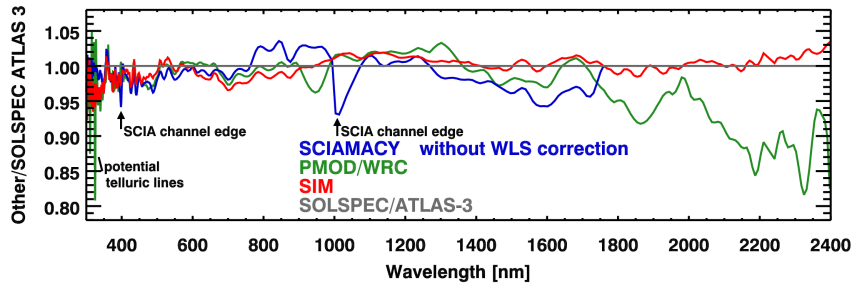


Fig. 3.2 SSI ratios of SCIAMACHY, SIM (Harder *et al.*, 2010), and PMOD/WRC (WRC85) composite (Wehrli, 1985) with respect to the SOLSPEC/ATLAS-3 shuttle experiment data (Thuillier *et al.*, 2004). Close to the channel boundaries of the SCIAMACHY instrument larger deviations are observed due to instrumental artifacts. From Pagaran *et al.* (2011a). Reproduced with permission ©ESO.

3.2 SCIAMACHY spectral solar irradiance

SCIAMACHY is a passive remote sensing double spectrometer combining a predispersing prism and eight gratings in separate channels. Silicon and InGaAs detectors are used as linear arrays with 1024 pixels each in Channels 1-5 (UV/visible) and Channels 6-8 (near IR), respectively. A detailed description of SCIAMACHY can be found in Bovensmann *et al.* (1999) and Pagaran *et al.* (2009).

Radiometrically calibrated SSI has been measured by SCIAMACHY since July 2002 once a day. A sample spectrum from March 2004 is shown in Fig. 3.1. The SCIAMACHY SSI has been compared with solar data from other satellites and measurements from the ground (Skupin *et al.*, 2005a,b; Pagaran *et al.*, 2011a). Figure 3.2 shows the comparison of SCIAMACHY with SIM (Harder *et al.*, 2010), the SOLSPEC/ATLAS-3 shuttle experiment (Thuillier *et al.*, 2004), and the PMOD/WRC (WRC85) composite (Wehrli, 1985). The PMOD/WRC composite (200 nm –10 μ m) was derived from various spectra obtained from aircraft, rocket, and balloon experiments as well as ground data from Neckel and Labs (1984). SCIAMACHY agrees to within 5% (SIM within 4%) with the SOLSPEC data from 300 to 1600 nm (Pagaran *et al.*, 2011a). The theoretical precision is usually in the range of 2-3% based upon radiometric standards (Bovensmann *et al.*, 1999). A more comprehensive comparison also to other solar data can be found in Pagaran *et al.* (2011a).

In later years of the SCIAMACHY mission the optical degradation in the UV due to the hard radiation environment in space is evident. The agreement of SCIAMACHY with other solar data can be improved when using the white light lamp (WLS) source as a degradation correction, however, the corrections are too strong since WLS itself is optically degrading and therefore this type of correction cannot be applied to the more recent SCIAMACHY data (Pagaran *et al.*, 2011a). Further investigations are underway to improve upon the in-flight radiometric calibration. For atmospheric studies this is generally not a problem since the degradation cancels out in the sun-normalized earth radiances used in most atmospheric retrievals.

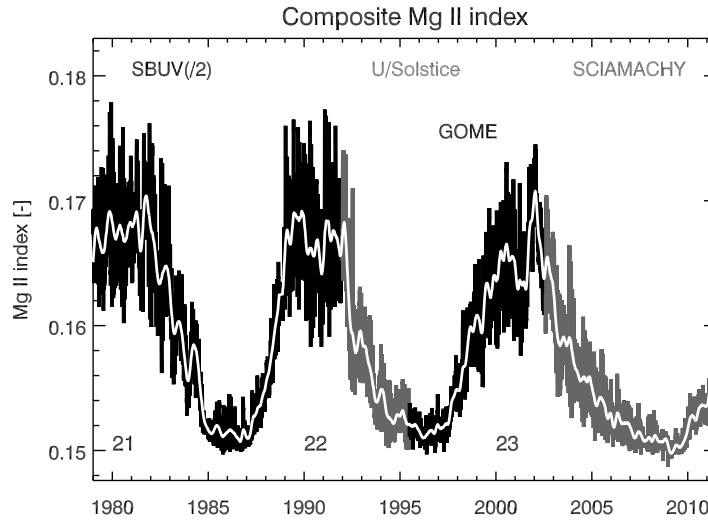


Fig. 3.3 Composite Mg II index measured near 280 nm derived from multiple satellite data and extending from solar cycle 21 to 24. In addition to SBUV(/2), UARS/Solstice, GOME, and SCIAMACHY as indicated here, other data such as SUSIM, the more recent SBUV/2 instruments from NOAA-16 to NOAA-18 as well as SORCE/Solstice have been used to fill daily gaps. The smooth white line shows the low-pass filtered time series by applying a 55-day triangular filter to remove the 27-day solar rotation signature.

The Mg II core to wing ratio derived from the Mg II Fraunhofer lines at 280 nm (Fig. 3.1) is an index that has been proven to correlate well with UV irradiance changes down to 30 nm (*DeLand and Cebula*, 1993; *Viereck et al.*, 2001). It is a measure for the chromospheric activity of the sun and describes the plage and faculae brightening responsible for the UV increase. The Mg II index, defined as a ratio, is insensitive to instrumental degradation and has been derived from many different instruments to provide a long-term time series going back to the late 1970s (*DeLand and Cebula*, 1993; *Viereck and Puga*, 1999; *Viereck et al.*, 2004). An updated composite Mg II index by adding the GOME (*Weber et al.*, 1998; *Weber*, 1999) and recent SCIAMACHY data is shown in Fig. 3.3. It seems that the Mg II index was lower during the recent solar minimum in 2008 than the two solar minima before, but this is not statistically significant. A potential lower solar minimum value could be expected from the very low thermospheric density observed in 2008 (*Emmert et al.*, 2010). Solar irradiance at extreme ultraviolet (EUV) wavelengths heats the thermosphere, causing it to expand. Low EUV irradiance contracts the thermosphere and decreases the density at a given altitude. The cooling of the upper atmosphere due to increases of greenhouse gases can only explain part of the recent contraction observed (*Emmert et al.*, 2010; *Solomon et al.*, 2011).

133 **3.3 Irradiance variations from solar rotations to several solar
134 cycles**

135 In order to estimate SSI irradiance variations beyond the instrument lifetime and
136 covering several decades a model was developed that uses solar proxies scaled to
137 SCIAMACHY SSI observations. The underlying assumption is that irradiance vari-
138 ations are mainly caused by solar surface magnetic activity (Fligge *et al.*, 2000) and
139 can be expressed in terms of faculae brightening as represented by the Mg II index
140 and sunspot darkening as expressed by the photometric sunspot index (PSI), here
141 taken from *Balmaceda et al.* (2009). The SSI can then be written as a time series as
142 follows

$$I_\lambda(t) = I_\lambda(t_0) + a_\lambda [P_a(t) - P_a(t_0)] + b_\lambda [P_b(t) - P_b(t_0)] + p_\lambda(t), \quad (3.1)$$

143 where $P_a(t)$ and $P_b(t)$ are the Mg II index and PSI time series, respectively. A similar
144 approach was used to model UV irradiance variations derived from UARS/Solstice
145 (*Lean et al.*, 1997).

146 A multivariate linear regression is performed to determine the regression coef-
147 ficients of the solar proxies. In addition to the two solar proxy terms piecewise
148 polynomials, $p_\lambda(t)$, are used to correct for instrument degradation and small jumps
149 following instrument and satellite platform anomalies (Pagaran *et al.*, 2009). The
150 regression was applied to SCIAMACHY SSI time series over several solar rotations
151 during 2003 and 2004. Regression coefficients, a_λ and b_λ , were determined from
152 240 nm to 1750 nm (SCIAMACHY channels 1 to 6) in steps of 10 nm (Pagaran
153 *et al.*, 2009). As a solar reference spectrum, $I_\lambda(t_0)$, the SCIAMACHY SSI from
154 March 4, 2004, (Fig. 3.1) was selected.

155 The modeled and observed SCIAMACHY solar irradiance change is shown as
156 an example in Fig. 3.4 during the Halloween 2003 solar storm, where the PSI index
157 value reached the lowest value since 1980 and substantial mesopsheric ozone loss
158 (mainly due to solar protons) was observed by SCIAMACHY (Rohen *et al.*, 2005).
159 The combined faculae and sunspot contributions and SCIAMACHY observations
160 are in qualitative agreement with Figure 6 in *Lean et al.* (2005). Across the near-
161 UV, vis, and near-IR spectral range solar irradiance dropped by 0.3% (near-IR) to
162 0.5% (near-UV). This is consistent with a drop of about 0.4% in the total solar
163 irradiance (TSI) or solar constant. Below 300 nm an irradiance enhancement due to
164 faculae activity was observed reaching +1.3% near 250 nm.

165 The SCIAMACHY irradiance timeseries as well as the SCIA proxy model show
166 the dark faculae effect in the spectral region 1400–1600 nm (near opacity H⁻ mini-
167 mum), where both sunspot and faculae contributions are negative in agreement with
168 observations from ground indicating a darkening under enhanced solar activity con-
169 ditions (Moran *et al.*, 1992). The SCIA proxy model, nevertheless, underestimates
170 the observed irradiance depletion in this spectral region.

171 The SCIA proxy model can be used to reconstruct spectral irradiance changes
172 since the late 1970s, where the Mg II index record started, covering nearly three
173 solar cycles. From the SCIA proxy model the UV contribution below 400 nm to TSI

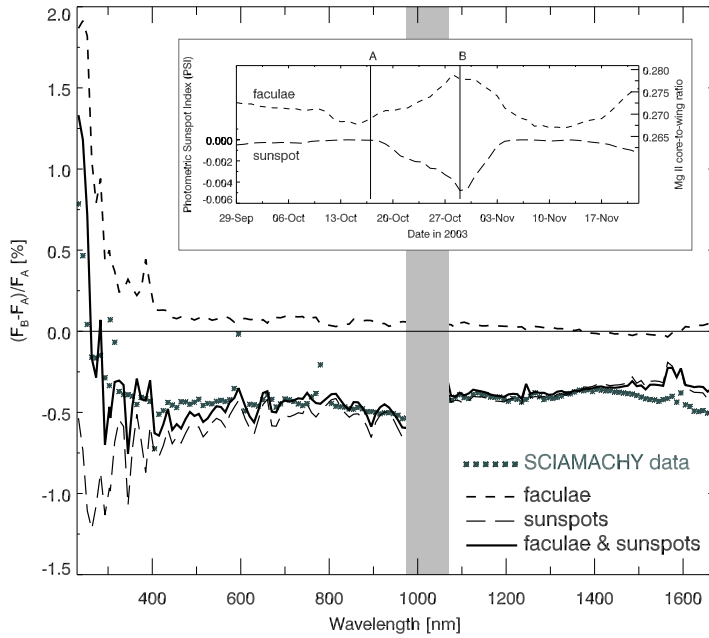


Fig. 3.4 Modeled and observed SCIAMACHY solar irradiance change during the Halloween solar storm in 2003 decomposed into faculae and sunspot contributions. The inset shows the Mg II and PSI index with labels A and B indicating dates from which irradiance differences were derived. From *Pagaran et al.* (2009). Reproduced by permission of the AAS.

174 changes in solar cycle 23 ($\sim 0.1\%$) is 55% (*Pagaran et al.*, 2009) which is higher
 175 than the 30% estimate from solar cycle 22 derived from SOLSTICE observations
 176 (*Lean et al.*, 1997) and lower than the 63% derived from the semi-empirical model
 177 SATIRE (Spectral and Total Irradiance Reconstructions) (*Krivova et al.*, 2006).

178 The largest TSI change contribution comes from the near UV (300–400 nm),
 179 where the irradiance solar cycle change per wavelength is well below 1% (*Pagaran*
 180 *et al.*, 2009). During solar cycles 21 to 23, the dominant contribution to irradiance
 181 changes in the UV from solar minimum to maximum comes from the faculae bright-
 182 ening. The sunspot contribution is non-negligible in the near UV and in the visible
 183 cancels within the error bars the faculae brightening (see Fig. 3.5, *Pagaran et al.*
 184 (2009, 2011b)). The dark faculae near 1400–1600 nm are again evident at solar
 185 maximum in agreement with observations by SIM and results from the SATIRE
 186 model (*Unruh et al.*, 2008).

187 *Harder et al.* (2009) reported on SIM irradiance changes during the descending
 188 phase of solar cycle 23 (April 2004 to November 2007) and found UV changes
 189 that are much larger than models like the NRLSSI irradiance model (*Lean*, 2000)
 190 indicate. This is also true when comparing to other data sets as shown in Fig. 3.6
 191 where the comparison is extended to the SCIA proxy model, the SATIRE model
 192 (*Krivova et al.*, 2009), and the UV composite from *DeLand and Cebula* (2008) as

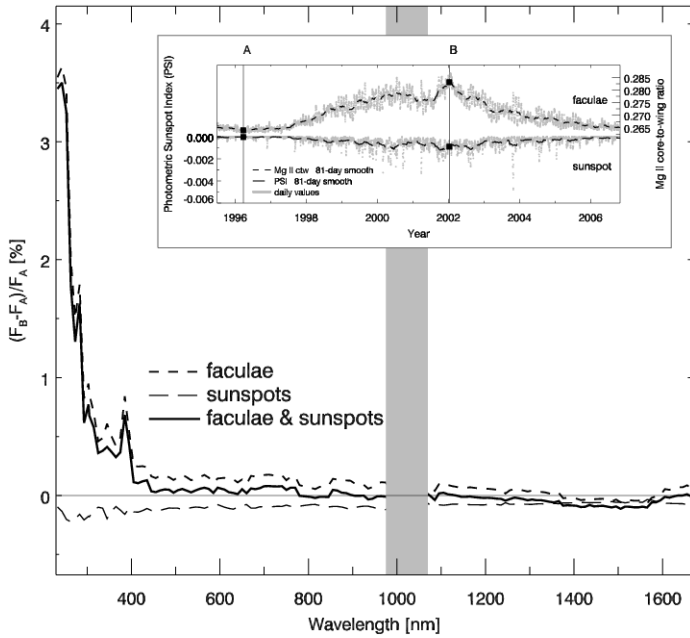


Fig. 3.5 Solar irradiance variations during solar cycle 23 as derived from SCIAMACHY observations and proxy data. Solar maximum and minimum dates were defined by the 81 day boxcar smooth of Mg II index timeseries (inset). Contributions from faculae and sunspots are indicated. From Pagaran *et al.* (2009). Reproduced by permission of the AAS.

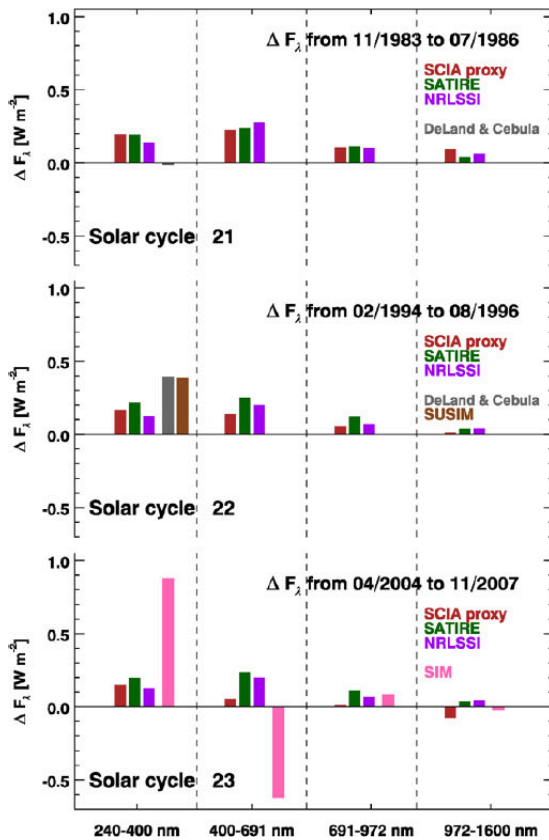
well. Also shown in this figure are the comparison of irradiance changes during the descending phase of prior solar cycles with similar Mg II index change as in solar cycle 23 (Pagaran *et al.*, 2011b).

It appears that current models including the SCIA proxy model that assume that irradiance changes are mostly related to surface magnetic activity are underestimating solar cycle changes in the UV as compared to the SIM observations. Direct observations from SUSIM and the UV composite also see larger UV changes during solar cycle 22 than the models, but are still only about half of SIM's result for solar cycle 23. Such a large UV change as observed by SIM has strong implications on radiative forcing in the upper atmosphere (Haigh *et al.*, 2010; Oberländer *et al.*, 2012) and will remain a matter of debate.

204 3.4 Solar rotation (27-day) signature in stratospheric ozone

205 The solar variation on the 11-year time scale has been shown to cause 2-3% variability
 206 in tropical ozone at altitudes of approximately 40 km. This has been concluded
 207 from different satellite observations (e.g. Remsberg, 2008; Fioletov, 2009, and ref-

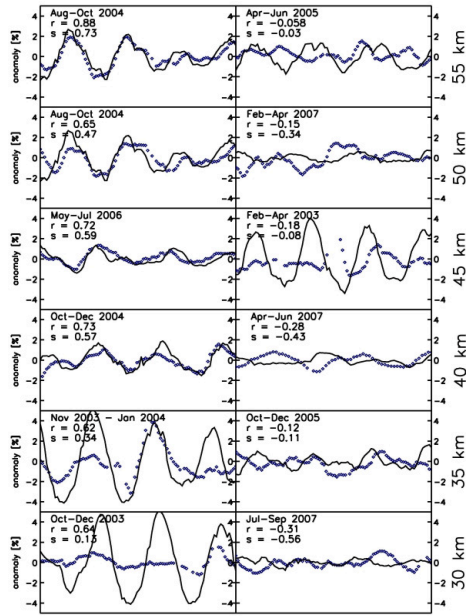
Fig. 3.6 SSI changes during part of the descending phase of solar cycles 21 to 23 (top to bottom), respectively. Dates near solar maximum and minimum are chosen in such a way that the differences between the Mg II indices are about the same in each solar cycle and correspond to that of the SIM observation period used here. NRLSSI (Lean, 2000), SATIRE (Krivova *et al.*, 2009) and SCIA proxy are models. SUSIM, SIM, and UV composite from DeLand and Cebula (2008) are direct satellite observations. From Pagaran *et al.* (2011b).



erences therein) and was confirmed by model studies (e.g. Langematz *et al.*, 2005; Sekiyama *et al.*, 2006; Marsh *et al.*, 2007). The influence of the 27-day solar rotation on ozone was first investigated by Hood (1986) in the 1980s using SBUV ozone measurements. He found the ozone sensitivity at 45 km to be slightly more than 0.4% per 1% change in the 205 nm flux. Further investigations with different satellite data sets and model outputs covering other time periods followed (Gruzdev *et al.*, 2009; Fioletov, 2009, and references therein). Austin *et al.* (2007) and Gruzdev *et al.* (2009) compared the 27-day ozone variability determined by chemistry climate models (CCM) with satellite measurements and were able to verify the observations in magnitude (0.4 to 0.5 %/%) but found the maximum ozone sensitivity slightly lower in altitude (approx. 40 km) in the model simulations.

The motivation for this study is to use the new dataset that is available from SCIAMACHY, e.g. global ozone profiles during the descending phase of solar cycle 23 (von Savigny *et al.*, 2005; Sonkaew *et al.*, 2009). Continuous wavelet transform (CWT), fast Fourier transform (FFT), and cross correlations (CC) have been applied to SCIAMACHY ozone in the tropics (<20° latitude) between 20 and 60 km altitude (Dikty *et al.*, 2010b). The maximum correlation between the Mg II index and ozone

Fig. 3.7 Selected three month periods with high (left panels) and low correlation (right panels) between ozone (solid line) and Mg II index (circles). In each panel, the period, correlation (r), and ozone sensitivity (s) is indicated, the latter is defined as the ozone change per Mg II index change in units of %/. The ozone sensitivity per unit 205 nm solar irradiance change is obtained by multiplying s with 0.61. From Dikty et al. (2010b). Reproduced by permission of American Geophysical Union. ©2010 American Geophysical Union.



is weaker during the maximum of solar cycle 23 ($r = 0.38$) than in the previous two solar cycles that have been investigated in earlier studies using different data sets. This is in agreement with results from Fioletov (2009).

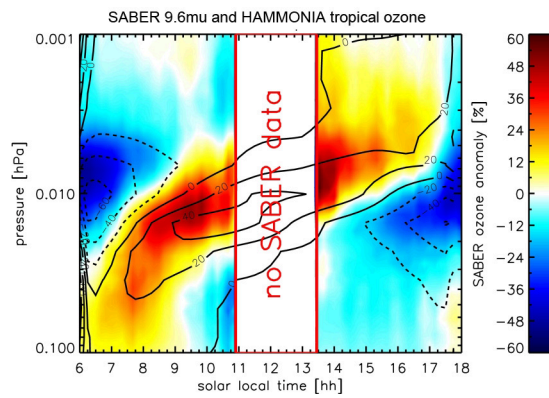
The magnitude of the ozone signals is highly time dependent as revealed by the CWT analysis and may vanish for several solar rotations even close to solar maximum conditions (see Fig. 3.7). The ozone sensitivity (ozone change in percent per percent change in 205 nm solar flux) is on average about 0.2%/% above 30 km altitude and smaller by about a factor of two compared to earlier studies. For selected three month periods the sensitivity may rise beyond 0.6%/% in better agreement with earlier studies. The analysis of the 27-day solar forcing was also carried out with stratospheric temperatures from the European Centre for Medium-Range Weather Forecasts operational analysis. Although direct radiation effects on temperature are weak in the upper stratosphere, temperature signals with statistically significant periods in the 25–35 day range similar to ozone were found (Dikty et al., 2010b).

3.5 Daytime variations in mesospheric ozone

In comparison with the 27-day solar rotation signal and the 11-year solar cycle response in the stratosphere, the diurnal and daytime variation of UV radiation inflicts a by far greater response in upper atmosphere ozone. The response of ozone above 60 km to variations in UV radiation is less well established. Ozone and temperature

245 data from SABER (Sounding of the Atmosphere using Broadband Emission Ra-
 246 diometry) in its version 1.07 (*Russell III et al.*, 1999) are used to study the daytime
 247 pattern of mesospheric ozone. In contrast to SCIAMACHY, SABER aboard TIMED
 248 flies in a more inclined orbit allowing measurements at different local times. In our
 249 study (*Dikty et al.*, 2010a) a specific sampling of SABER data was preformed to de-
 250 rive daytime pattern in tropical ozone using both the results from the $1.27\mu\text{m}$ air glow
 251 (*Mlynczak et al.*, 2007) and $9.6\mu\text{m}$ thermal emission retrieval (*Rong et al.*, 2008).
 252 Compared to the earlier study on daytime variations by *Huang et al.* (2008) more
 253 years of SABER data were used and our results were compared to HAMMONIA
 254 (Hamburg Model of the Neutral and Ionized Atmosphere) (*Schmidt et al.*, 2006).

Fig. 3.8 SABER observations at $9.6\mu\text{m}$ (color) and HAMMONIA model (contour) daytime ozone variations between 0.1 and 0.001 hPa expressed as percent deviation from the daytime mean. From *Dikty et al.* (2010a).



255 The amplitude of daytime ozone variations is approximately 60% of the day-
 256 time mean for SABER and lower for the model (see Fig. 3.8). The agreement
 257 with HAMMONIA is generally better for the $9.6\mu\text{m}$ retrieved ozone data than for
 258 the $1.27\mu\text{m}$ air glow retrieval (*Dikty et al.*, 2010a). The maximum daytime peak
 259 anomaly observed at 0.05 hPa (~ 70 km) in the morning shifts its altitude to about
 260 0.007 hPa (~ 80 km) in the afternoon. This daytime shift is in very good agreement
 261 with the model, however the peak anomaly reaches a maximum of 40–50% of the
 262 daytime mean, which is higher than HAMMONIA (30–40%). Negative anomalies
 263 are observed in the early morning hours at 0.007 hPa and in the late afternoon near
 264 0.015 hPa in quite good agreement with the model. During equinox the daytime
 265 maximum ozone abundance is higher than during solstice, especially above 0.01 hPa
 266 (approx. 80 km). The seasonal variation is somewhat weaker in HAMMONIA.

267 In contrast to ozone, temperature data from SABER (*Remsberg et al.*, 2008) show
 268 little daytime variations between 65 and 90 km and their amplitudes are less than
 269 1.5%, suggesting photochemistry playing a dominant role in the mesospheric ozone
 270 chemistry. *Marsh et al.* (2002) proposed that the solar diurnal tide brings down
 271 atomic oxygen for ozone production in the afternoon (> 85 km). The model, how-
 272 ever, underestimates ozone in the afternoon above approximately 0.01 hPa, so the
 273 remaining difference could be attributed to solar tides. The minimum early in the
 274 morning is caused by the direct photolysis of ozone before enough atomic oxy-

275 gen is produced to counteract the ozone destruction. The ozone rise in the morning
 276 hours may also be due to tides transporting ozone rich air from below (*Marsh et al.*,
 277 2002). The new SABER version 1.08 data will also include water vapor, which will
 278 be helpful to constrain the HO_x budget and its influence on daytime ozone.

279 3.6 Conclusion

280 SCIAMACHY was the first satellite instrument providing daily spectral solar irradi-
 281 ances (SSI) from the UV, visible and near infrared. The comparisons with other solar
 282 data from space and ground showed good agreement to within a few percent up to
 283 1700 nm (*Skupin et al.*, 2005a,b; *Pagaran et al.*, 2011a). Expressing SCIAMACHY
 284 irradiance variations over several solar rotations in terms of solar proxies for sunspot
 285 darkening and faculae brightening permits the extrapolation of SCIAMACHY SSI
 286 variations to the 11-year solar cycle scales (*Pagaran et al.*, 2009, 2011b). It was
 287 shown that about half of the 0.1% change in the solar constant over solar cycle
 288 23 has originates from the visible and IR spectral region (*Pagaran et al.*, 2009). A
 289 particular challenge is the solar cycle variation estimate for the near UV (300-400
 290 nm), where recent SIM observations (*Harder et al.*, 2009) indicate changes during
 291 solar cycle 23 that are much higher than expected from indirect SCIAMACHY ob-
 292 servations and other empirical models (assuming solar surface magnetic activity as
 293 primary driver for SSI variations) as well as observations from other satellite data in
 294 earlier solar cycles (*Pagaran et al.*, 2011b).

295 SCIAMACHY limb ozone vertical profiles from 2003 to 2008 were analyzed for
 296 signatures of the 27-day solar rotation. It was found that this signature is highly
 297 variable in time and that even under solar maximum condition this signal can vanish
 298 for several months (*Dikty et al.*, 2010b). On average the sensitivity above 30 km is a
 299 0.2% ozone change per percent change in the 205 nm solar flux (important for ozone
 300 production) near solar maximum, which is smaller than found in earlier studies and
 301 prior solar cycles.

302 Daytime variations in tropical mesospheric ozone yield changes of up to 60%
 303 from the daytime mean based upon SABER ozone data and peak anomalies are gen-
 304 erally higher during equinox. SABER results were compared for the first time with
 305 an output of a chemistry climate model, here the HAMMONIA model (*Dikty et al.*,
 306 2010a). SABER ozone from the 9.6 μ m retrieval agrees qualitatively very well with
 307 HAMMONIA, however, little agreement was found between modeled and SABER
 308 temperatures above 0.01 hPa. The low temperature variations of a few degree during
 309 daytime may suggest that photochemical processes are the main driver for daytime
 310 ozone variations and to a lesser degree transport related to tides.

311 **Acknowledgements** The support by the DFG research project SOLOZON (DFG WE 3647/1-1)
 312 within the German CAWSES priority program and the support by the State of Bremen is gratefully
 313 acknowledged. The authors JP, MW, LEF, and GWH were part of the International Space Studies

314 Institute (ISSI) team on spectral solar irradiance (<http://www.issibern.ch/teams/solarspect/>), whose
315 meetings and discussions have greatly benefitted this work.

316 **References**

- 317 Austin, J., L. L. Hood, and B. E. Soukharev (2007), Solar cycle variations of strato-
318 ospheric ozone and temperature in simulations of a coupled chemistry-climate
319 model, *Atmos. Chem. Phys.*, **7**, 1693–1706.
320 Balmaceda, L. A., S. K. Solanki, N. A. Krivova, and S. Foster (2009), A homoge-
321 neous sunspot areas database covering more than 130 years, *J. Geophys. Res.*,
322 **114**, A7104, doi:10.1029/2009JA014299.
323 Bovensmann, H., J. P. Burrows, M. Buchwitz, J. Frerick, S. Noël, V. V. Rozanov,
324 K. V. Chance, and A. P. H. Goede (1999), SCIAMACHY: Mission objectives and
325 measurement modes, *J. Atmos. Sci.*, **56**, 127–150.
326 Bovensmann, H., I. Aben, M. van Roozendael, S. Kühl, M. Gottwald, C. von Savigny,
327 M. Buchwitz, A. Richter, C. Frankenberg, P. Stammes, M. de Graaf, F. Wittrock,
328 M. Sinnhuber, B.-M. Sinnhuber, A. Schönhardt, S. Beirle, A. Gloudemann,
329 H. Schrijver, A. Bracher, A. V. Rozanov, M. Weber, and J. P. Burrows
330 (2011), SCIAMACHY's view of the changing earth's environment, in *SCIA-
331 MACHY - Exploring the Changing Earth's Atmosphere*, edited by M. Gottwald
332 and H. Bovensmann, chap. 10, Springer, Dordrecht, doi:10.1007/978-90-481-
333 9896-2.
334 Burrows, J. P., M. Weber, M. Buchwitz, V. Rozanov, A. Ladstätter-Weißenmayer,
335 A. Richter, R. Debeek, R. Hoogen, K. Bramstedt, K.-U. Eichmann, M. Eisinger,
336 and D. Perner (1999), The Global Ozone Monitoring Experiment (GOME): Mis-
337 sion concept and first scientific results, *J. Atmos. Sci.*, **56**, 151–175.
338 DeLand, M. T., and R. P. Cebula (1993), Composite Mg II solar activity index for
339 solar cycles 21 and 22, *J. Geophys. Res.*, **98**, 12,809–12,823.
340 DeLand, M. T., and R. P. Cebula (2008), Creation of a composite solar ultraviolet
341 irradiance data set, *J. Geophys. Res.*, **113**, A11,103, doi:10.1029/2008JA013401.
342 DeLand, M. T., L. E. Floyd, G. J. Rottman, and J. Pap (2004), Status of UARS solar
343 UV irradiance data, *Adv. Space Res.*, **34**, 243–250.
344 Dikty, S., H. Schmidt, M. Weber, C. von Savigny, and M. G. Mlynczak (2010a),
345 Daytime ozone and temperature variations in the mesosphere: a comparison be-
346 tween SABER observations and HAMMONIA model, *Atmos. Chem. Phys.*, **10**,
347 8331–8339, doi:10.5194/acp-10-8331-2010.
348 Dikty, S., M. Weber, C. von Savigny, T. Sonkaew, A. Rozanov, and J. P. Burrows
349 (2010b), Modulations of the 27-day solar cycle signal in stratospheric ozone from
350 SCIAMACHY, *J. Geophys. Res.*, **115**, D00,115, doi:10.1029/2009JD012379.
351 Emmert, J. T., J. L. Lean, and J. M. Picone (2010), Record-low thermospheric
352 density during the 2008 solar minimum, *Geophys. Res. Lett.*, **37**, L12,102, doi:
353 10.1029/2010GL043671.

- 354 Fioletov, V. E. (2009), Estimating the 27-day and 11-year solar cycle variations
355 in tropical upper stratospheric ozone, *J. Geophys. Res.*, **114**, D02,302, doi:
356 10.1029/2008JD010499.
- 357 Fligge, M., S. K. Solanki, and Y. C. Unruh (2000), Modelling irradiance variations
358 from the surface distribution of the solar magnetic field, *Astron. Astrophys.*, **353**,
359 380–388.
- 360 Fröhlich, C., C. A. Crommelynck, C. Wehrli, M. Anklin, S. Dewitte, A. Fichot,
361 W. Finsterle, A. Jiménez, A. Chevalier, and H. Roth (1997), In-flight performance
362 of the Virgo solar irradiance instruments on SOHO, *Sol. Phys.*, **175**, 267–286.
- 363 Gruzdev, A. N., H. Schmidt, and G. P. Brasseur (2009), The effect of the solar
364 rotational irradiance variation on the middle and upper atmosphere calculated
365 by a three-dimensional chemistry-climate model, *Atmos. Chem. Phys.*, **8**, 1113–
366 1158.
- 367 Haigh, J. D., A. R. Winning, R. Toumi, and J. W. Harder (2010), An influence of
368 solar spectral variations on radiative forcing of climate, *Nature*, **467**, 696–699,
369 doi:10.1038/nature09426.
- 370 Harder, J. W., G. Lawrence, J. Fontenla, G. Rottman, and T. Woods (2005a), The
371 Spectral Irradiance Monitor: Scientific requirements, instrument design, and op-
372 eration modes, *Sol. Phys.*, **230**, 141–167, doi:10.1007/s11207-005-5007-5.
- 373 Harder, J. W., J. Fontenla, G. Lawrence, T. Woods, and G. Rottman (2005b), The
374 Spectral Irradiance Monitor: Measurement equations and calibration, *Sol. Phys.*,
375 **230**, 169–204, doi:10.1007/s11207-005-1528-1.
- 376 Harder, J. W., J. M. Fontenla, P. Pilewskie, E. C. Richard, and T. N. Woods (2009),
377 Trends in solar spectral irradiance variability in the visible and infrared, *Geophys.
378 Res. Lett.*, **36**, 7801, doi:10.1029/2008GL036797.
- 379 Harder, J. W., G. Thuillier, E. C. Richard, S. W. Brown, K. R. Lykke, M. Snow,
380 W. E. McClintock, J. M. Fontenla, T. N. Woods, and P. Pilewskie (2010), The
381 SORCE SIM solar spectrum: Comparison with recent observations, *Sol. Phys.*,
382 **263**, 3–24, doi:10.1007/s11207-010-9555-y.
- 383 Hood, L. L. (1986), Coupled stratospheric ozone and temperature response to short-
384 term changes in solar ultraviolet flux: An analysis of Nimbus 7 SBUV and SAMS
385 data, *J. Geophys. Res.*, **91**, 5264s–5276.
- 386 Huang, F. T., H. Mayr, J. M. Russell III, M. G. Mlynczak, and C. A. Reber (2008),
387 Ozone diurnal variations and mean profiles in the mesosphere, lower thermo-
388 sphere, and stratosphere, based on measurements from SABER on TIMED, *J.
389 Geophys. Res.*, **113**, A04,307, doi:10.1029/2007JA012739.
- 390 Krivova, N. A., S. K. Solanki, and L. Floyd (2006), Reconstruction of solar
391 uv irradiance in cycle 23, *Astron. Astrophys.*, **452**, 631–639, doi:10.1051/0004-
392 6361:20064809.
- 393 Krivova, N. A., S. K. Solanki, T. Wenzler, and B. Podlipnik (2009), Reconstruc-
394 tion of solar UV irradiance since 1974, *J. Geophys. Res.*, **114**, D00I04, doi:
395 10.1029/2009JD012375.
- 396 Langematz, U., J. L. Grenfell, K. Matthes, P. Mieth, M. Kunze, B. Steil, and C. Brühl
397 (2005), Chemical effects in 11-year solar cycle simulations with the Freie Uni-

- 398 versität Berlin Middle Atmospheric Model with online chemistry (FUB-CMAM-
399 CHEM), *Geophys. Res. Lett.*, 32(L13803), doi:10.1029/2005GL022686.
400 Lean, J., G. Rottman, J. Harder, and G. Kopp (2005), SORCE contributions to new
401 understanding of global change and solar variability, *Sol. Phys.*, 230, 27–53, doi:
402 10.1007/s11207-005-1527-2.
403 Lean, J. L. (2000), Evolution of the sun's spectral irradiance since the Maunder
404 minimum, *Geophys. Res. Lett.*, 16, 2425–2428.
405 Lean, J. L., G. J. Rottman, H. L. Kyle, T. N. Woods, J. R. Hickey, and L. C.
406 Puga (1997), Detection and parameterization of variations in solar mid- and near-
407 ultraviolet radiation (200–400 nm), *J. Geophys. Res.*, 102, 29,939–29,956.
408 Marsh, D. R., W. R. Skinner, A. R. Marshall, P. B. Hays, D. A. Ortland, and
409 J.-H. Yee (2002), High Resolution Doppler Imager observations of ozone in
410 the mesosphere and lower thermosphere, *J. Geophys. Res.*, 107, 4390, doi:
411 10.1029/2001JD001505.
412 Marsh, D. R., R. R. Garcia, D. E. Kinnison, B. A. Boville, F. Sassi, S. C. Solomon,
413 and K. Matthes (2007), Modelling the whole atmosphere response to solar cycle
414 changes in radiative and geomagnetic forcing, *J. Geophys. Res.*, 112(D23306),
415 doi:10.1029/2006JD008306.
416 Mlynczak, M. G., B. T. Marshall, F. J. Martin-Torres, J. M. Russel III, R. E.
417 Thompson, E. E. Remsberg, and L. L. Gordley (2007), Sounding of the Atmo-
418 sphere using Broadband Emission Radiometry observations of daytime meso-
419 stratospheric O₂(¹Δ) 1.27 μm emission and derivation of ozone, atomic oxygen, and
420 solar and chemical energy deposition rates, *J. Geophys. Res.*, 112, D15,306, doi:
421 10.1029/2006JD008355.
422 Moran, T., P. Foukal, and D. Rabin (1992), A photometric study of faculae and
423 sunspots between 1.2 and 1.6 micron, *Sol. Phys.*, 142, 35–46.
424 Neckel, H., and D. Labs (1984), The solar radiation between 3300 and 12500 Å, *Sol.*
425 *Phys.*, 90, 205–258.
426 Oberländer, S., U. Langematz, K. Matthes, M. Kunze, A. Kubin, J. Harder, N. A.
427 Krivova, S. K. Solanki, J. Pagaran, and M. Weber (2012), The influence of spec-
428 tral solar irradiance data on stratospheric heating rates during the 11 year solar
429 cycle, *Geophys. Res. Lett.*, 39, L01,801, doi:10.1029/2011GL049539.
430 Pagaran, J., M. Weber, and J. P. Burrows (2009), Solar variability from 240 to 1750
431 nm in terms of faculae brightening and sunspot darkening from SCIAMACHY,
432 *Astron. J.*, 700, 1884–1895.
433 Pagaran, J., G. Harder, M. Weber, L. Floyd, and J. P. Burrows (2011a), Intercom-
434 parison of SCIAMACHY and SIM vis-IR irradiance over several solar rotational
435 timescales, *Astron. Astrophys.*, 528, A67, doi:10.1051/0004-6361/201015632.
436 Pagaran, J., M. Weber, M. DeLand, L. Floyd, and J. P. Burrows (2011b), Solar spec-
437 tral irradiance variations in 240–1600 nm during the recent solar cycles 21–23,
438 *Sol. Phys.*, XX, XX–XX.
439 Remsberg, E. E. (2008), On the response of Halogen Occultation Experiment
440 (HALOE) stratospheric ozone and temperature to the 11-year solar cycle forc-
441 ing, *J. Geophys. Res.*, 113(D22304), doi:10.1029/2008JD010189.

- 442 Remsberg, E. E., B. T. Marshall, M. Garcia-Comas, D. Krueger, G. S. Lingen-
 443 felser, J. Martin-Torres, M. G. Mlynczak, J. M. Russel III, A. K. Smith, Y. Zhao,
 444 C. Brown, L. L. Gordley, M. J. Lopez-Gonzales, M. Lopez-Puertas, C.-Y. She,
 445 M. J. Taylor, and R. E. Thompson (2008), Assement of the quality of the Ver-
 446 sion 1.07 temperature-versus-pressure profiles of the middle atmosphere from
 447 TIMED/SABER, *J. Geophys. Res.*, *113*, D17,101, doi:10.1029/2008JD010013.
- 448 Rohen, G., C. von Savigny, M. Sinnhuber, E. J. Llewellyn, J. W. Kaiser, C. H.
 449 Jackman, M.-B. Kallenrode, J. Schröter, K.-U. Eichmann, H. Bovensmann, and
 450 J. P. Burrows (2005), Ozone depletion during the solar proton events of Octo-
 451 ber/November 2003 as seen by SCIAMACHY, *J. Geophys. Res.*, *110*, A09S39,
 452 doi:10.1029/2004JA010984.
- 453 Rong, P. P., J. M. Russell III, M. G. Mlynczak, E. E. Remsberg, B. T. Marshall,
 454 L. L. Gordley, and M. Lopez-Puertas (2008), Validation of TIMED/SABER v1.07
 455 ozone at 9.6 μm in the altitude range 15–70 km, *J. Geophys. Res.*, *114*, D04,306,
 456 doi:10.1029/2008JD010073.
- 457 Rottman, G., L. Floyd, and R. Viereck (2004), Measurement of solar ultraviolet
 458 irradiance, *Geophys. Mono.*, *41*, 111–125, doi:10.10219/141GM10.
- 459 Russell III, J. M., M. G. Mlynczak, L. L. Gordley, J. J. Tansock Jr., and R. W. Esplin
 460 (1999), Overview of the SABER experiment and preliminary calibration results,
 461 *Proc. SPIE*, *3756*(277), doi:10.1117/12.366382.
- 462 Schmidt, H., G. P. Brasseur, M. Charron, E. Manzini, M. A. Giorgetta, T. Diehl,
 463 V. I. Fomichev, D. Kinnison, D. Marsh, and S. Walters (2006), The HAMMONIA
 464 Chemistry climate model: Sensitivity of the mesopause region to the 11-year solar
 465 cycle and CO₂ doubling, *J. Climate*, *19*, 3903–3931.
- 466 Sekiyama, T. T., K. Shibata, M. Deushi, K. Kodera, and J. L. Lean (2006), Strato-
 467 spheric ozone variation induced by the 11-year solar cycle: Recent 22-year sim-
 468 ulation using 3-D chemical transport model with reanalysis data, *Geophys. Res.
 469 Lett.*, *33*(L17812), doi:10.1029/2006GL026711.
- 470 Skupin, J., S. Noël, M. W. Wuttke, M. Gottwald, H. Bovensmann, M. We-
 471 ber, and J. P. Burrows (2005a), SCIAMACHY solar irradiance observation in
 472 the spectral range from 240 to 2380 nm, *Adv. Space Res.*, *35*, 370–375, doi:
 473 10.1016/j.asr.2005.03.036.
- 474 Skupin, J., M. Weber, S. Noël, H. Bovensmann, and J. P. Burrows (2005b), GOME
 475 and SCIAMACHY solar measurements: Solar spectral irradiance and Mg II solar
 476 activity proxy indicator, *Mem. Soc. Astron. Ital.*, *76*, 1038–1041.
- 477 Solomon, S. C., L. Qian, L. V. Didkovsky, R. A. Viereck, and T. N. Woods (2011),
 478 Causes of low thermospheric density during the 2007–2009 solar minimum, *J.
 479 Geophys. Res.*, *116*, doi:10.1029/2011JA016508, in press.
- 480 Sonkaew, T., V. V. Rozanov, C. von Savigny, A. Rozanov, H. Bovensmann, and
 481 J. P. Burrows (2009), Cloud sensitivity studies for stratospheric and lower meso-
 482 spheric ozone profile retrievals from measurements of limb scattered solar radia-
 483 tion, *Atmos. Meas. Tech.*, *2*, 653–678, doi:10.5194/amt-2-653-2009.
- 484 Thuillier, G., L. Floyd, T. N. Woods, R. Cebula, E. Hilsenrath, M. Hersé, and
 485 D. Labs (2004), Solar irradiance reference spectra, in *Solar Variability and its
 486 Effects on Climate. Geophysical Monograph 141*, vol. 141, edited by J. M. Pap,

- 487 P. Fox, C. Fröhlich, J. K. H. S. Hudson, J. McCormack, G. North, W. Sprigg, and
488 S. T. Wu, pp. 171–194.
- 489 Unruh, Y. C., N. A. Krivova, S. K. Solanki, J. W. Harder, and G. Kopp (2008),
490 Spectral irradiance variations: comparison between observations and the SATIRE
491 model on solar rotation time scales, *Astron. Astrophys.*, **486**, 311–323, doi:
492 10.1051/0004-6361:20078421.
- 493 Viereck, R. A., and L. C. Puga (1999), The NOAA Mg II core-to-wing solar index:
494 Construction of a 20-year times series of chromospheric variability from multiple
495 satellites, *J. Geophys. Res.*, **104**, 9,995–10,005.
- 496 Viereck, R. A., L. Puga, D. McMullin, D. Judge, M. Weber, and W. K. Tobiska
497 (2001), The Mg II index: A proxy for solar EUV, *Geophys. Res. Lett.*, **28**, 1343–
498 1346.
- 499 Viereck, R. A., L. E. Floyd, P. C. Crane, T. Woods, B. G. Knapp, G. Rottman,
500 M. Weber, L. C. Puga, and M. T. DeLand (2004), A composite Mg II index span-
501 ning from 1978 to 2003, *Space Weather*, **2**, S10,005.
- 502 von Savigny, C., A. Rozanov, H. Bovensmann, K.-U. Eichmann, S. Noël, V. V.
503 Rozanov, M. Weber, J. P. Burrows, and J. W. Kaiser (2005), The ozone hole
504 breakup in September 2002 as seen by SCIAMACHY on ENVISAT, *J. Atmos.
505 Sci.*, **62**, 721–734.
- 506 Weber, M. (1999), Solar Activity during solar cycle 23 monitored by GOME,
507 in *ESA-WPP 1999: European Symposium on Atmospheric Measurements from
508 Space, Proc. ESAMS '99, ESA Special Publication*, vol. 161, pp. 611–616, ESA
509 Publications Division, Nordwijk.
- 510 Weber, M., J. P. Burrows, and R. P. Cebula (1998), GOME solar uv/vis irradiance
511 measurements between 1995 and 1997 - First results on proxy solar activity stud-
512 ies, *Sol. Phys.*, **177**, 63–77.
- 513 Wehrli, C. (1985), Extraterrestrial solar spectrum, *Tech. rep.*, Physikalisch-
514 Meteorologisches Observatorium, World Radiation Center (PMO/WRC), Publi-
515 cation No. 615.

516 References

- 517 Austin, J., L. L. Hood, and B. E. Soukharev (2007), Solar cycle variations of strato-
518 ospheric ozone and temperature in simulations of a coupled chemistry-climate
519 model, *Atmos. Chem. Phys.*, 7, 1693–1706.
- 520 Balmaceda, L. A., S. K. Solanki, N. A. Krivova, and S. Foster (2009), A homoge-
521 neous sunspot areas database covering more than 130 years, *J. Geophys. Res.*,
522 114, A7104, doi:10.1029/2009JA014299.
- 523 Bovensmann, H., J. P. Burrows, M. Buchwitz, J. Frerick, S. Noël, V. V. Rozanov,
524 K. V. Chance, and A. P. H. Goede (1999), SCIAMACHY: Mission objectives and
525 measurement modes, *J. Atmos. Sci.*, 56, 127–150.
- 526 Bovensmann, H., I. Aben, M. van Roozendael, S. Kühl, M. Gottwald, C. von Savigny,
527 M. Buchwitz, A. Richter, C. Frankenberg, P. Stammes, M. de Graaf, F. Wit-
528 trock, M. Sinnhuber, B.-M. Sinnhuber, A. Schönhardt, S. Beirle, A. Gloude-
529 mans, H. Schrijver, A. Bracher, A. V. Rozanov, M. Weber, and J. P. Burrows
530 (2011), SCIAMACHY's view of the changing earth's environment, in *SCIA-
531 MACHY - Exploring the Changing Earth's Atmosphere*, edited by M. Gottwald
532 and H. Bovensmann, chap. 10, Springer, Dordrecht, doi:10.1007/978-90-481-
533 9896-2.
- 534 Burrows, J. P., M. Weber, M. Buchwitz, V. Rozanov, A. Ladstätter-Weißenmayer,
535 A. Richter, R. Debeek, R. Hoogen, K. Bramstedt, K.-U. Eichmann, M. Eisinger,
536 and D. Perner (1999), The Global Ozone Monitoring Experiment (GOME): Mis-
537 sion concept and first scientific results, *J. Atmos. Sci.*, 56, 151–175.
- 538 DeLand, M. T., and R. P. Cebula (1993), Composite Mg II solar activity index for
539 solar cycles 21 and 22, *J. Geophys. Res.*, 98, 12,809–12,823.
- 540 DeLand, M. T., and R. P. Cebula (2008), Creation of a composite solar ultraviolet
541 irradiance data set, *J. Geophys. Res.*, 113, A11,103, doi:10.1029/2008JA013401.
- 542 DeLand, M. T., L. E. Floyd, G. J. Rottman, and J. Pap (2004), Status of UARS solar
543 UV irradiance data, *Adv. Space Res.*, 34, 243–250.
- 544 Dikty, S., H. Schmidt, M. Weber, C. von Savigny, and M. G. Mlynczak (2010a),
545 Daytime ozone and temperature variations in the mesosphere: a comparison be-
546 tween SABER observations and HAMMONIA model, *Atmos. Chem. Phys.*, 10,
547 8331–8339, doi:10.5194/acp-10-8331-2010.
- 548 Dikty, S., M. Weber, C. von Savigny, T. Sonkaew, A. Rozanov, and J. P. Burrows
549 (2010b), Modulations of the 27-day solar cycle signal in stratospheric ozone from
550 SCIAMACHY, *J. Geophys. Res.*, 115, D00,115, doi:10.1029/2009JD012379.
- 551 Emmert, J. T., J. L. Lean, and J. M. Picone (2010), Record-low thermospheric
552 density during the 2008 solar minimum, *Geophys. Res. Lett.*, 37, L12,102, doi:
553 10.1029/2010GL043671.
- 554 Fioletov, V. E. (2009), Estimating the 27-day and 11-year solar cycle variations
555 in tropical upper stratospheric ozone, *J. Geophys. Res.*, 114, D02,302, doi:
556 10.1029/2008JD010499.
- 557 Fligge, M., S. K. Solanki, and Y. C. Unruh (2000), Modelling irradiance variations
558 from the surface distribution of the solar magnetic field, *Astron. Astrophys.*, 353,
559 380–388.

- 560 Fröhlich, C., C. A. Crommelynck, C. Wehrli, M. Anklin, S. Dewitte, A. Fichot,
561 W. Finsterle, A. Jiménez, A. Chevalier, and H. Roth (1997), In-flight performance
562 of the Virgo solar irradiance instruments on SOHO, *Sol. Phys.*, **175**, 267–286.
- 563 Gruzdev, A. N., H. Schmidt, and G. P. Brasseur (2009), The effect of the solar
564 rotational irradiance variation on the middle and upper atmosphere calculated
565 by a three-dimensional chemistry-climate model, *Atmos. Chem. Phys.*, **8**, 1113–
566 1158.
- 567 Haigh, J. D., A. R. Winning, R. Toumi, and J. W. Harder (2010), An influence of
568 solar spectral variations on radiative forcing of climate, *Nature*, **467**, 696–699,
569 doi:10.1038/nature09426.
- 570 Harder, J. W., G. Lawrence, J. Fontenla, G. Rottman, and T. Woods (2005a), The
571 Spectral Irradiance Monitor: Scientific requirements, instrument design, and op-
572 eration modes, *Sol. Phys.*, **230**, 141–167, doi:10.1007/s11207-005-5007-5.
- 573 Harder, J. W., J. Fontenla, G. Lawrence, T. Woods, and G. Rottman (2005b), The
574 Spectral Irradiance Monitor: Measurement equations and calibration, *Sol. Phys.*,
575 **230**, 169–204, doi:10.1007/s11207-005-1528-1.
- 576 Harder, J. W., J. M. Fontenla, P. Pilewskie, E. C. Richard, and T. N. Woods (2009),
577 Trends in solar spectral irradiance variability in the visible and infrared, *Geophys.
578 Res. Lett.*, **36**, 7801, doi:10.1029/2008GL036797.
- 579 Harder, J. W., G. Thuillier, E. C. Richard, S. W. Brown, K. R. Lykke, M. Snow,
580 W. E. McClintock, J. M. Fontenla, T. N. Woods, and P. Pilewskie (2010), The
581 SORCE SIM solar spectrum: Comparison with recent observations, *Sol. Phys.*,
582 **263**, 3–24, doi:10.1007/s11207-010-9555-y.
- 583 Hood, L. L. (1986), Coupled stratospheric ozone and temperature response to short-
584 term changes in solar ultraviolet flux: An analysis of Nimbus 7 SBUV and SAMS
585 data, *J. Geophys. Res.*, **91**, 5264s–5276.
- 586 Huang, F. T., H. Mayr, J. M. Russell III, M. G. Mlynczak, and C. A. Reber (2008),
587 Ozone diurnal variations and mean profiles in the mesosphere, lower thermo-
588 sphere, and stratosphere, based on measurements from SABER on TIMED, *J.
589 Geophys. Res.*, **113**, A04,307, doi:10.1029/2007JA012739.
- 590 Krivova, N. A., S. K. Solanki, and L. Floyd (2006), Reconstruction of solar
591 uv irradiance in cycle 23, *Astron. Astrophys.*, **452**, 631–639, doi:10.1051/0004-
592 6361:20064809.
- 593 Krivova, N. A., S. K. Solanki, T. Wenzler, and B. Podlipnik (2009), Reconstruc-
594 tion of solar UV irradiance since 1974, *J. Geophys. Res.*, **114**, D00I04, doi:
595 10.1029/2009JD012375.
- 596 Langematz, U., J. L. Grenfell, K. Matthes, P. Mieth, M. Kunze, B. Steil, and C. Brühl
597 (2005), Chemical effects in 11-year solar cycle simulations with the Freie Uni-
598 versität Berlin Middle Atmospheric Model with online chemistry (FUB-CMAM-
599 CHEM), *Geophys. Res. Lett.*, **32**(L13803), doi:10.1029/2005GL022686.
- 600 Lean, J., G. Rottman, J. Harder, and G. Kopp (2005), SORCE contributions to new
601 understanding of global change and solar variability, *Sol. Phys.*, **230**, 27–53, doi:
602 10.1007/s11207-005-1527-2.
- 603 Lean, J. L. (2000), Evolution of the sun's spectral irradiance since the Maunder
604 minimum, *Geophys. Res. Lett.*, **16**, 2425–2428.

- 605 Lean, J. L., G. J. Rottman, H. L. Kyle, T. N. Woods, J. R. Hickey, and L. C.
 606 Puga (1997), Detection and parameterization of variations in solar mid- and near-
 607 ultraviolet radiation (200-400 nm), *J. Geophys. Res.*, *102*, 29,939–29,956.
- 608 Marsh, D. R., W. R. Skinner, A. R. Marshall, P. B. Hays, D. A. Ortland, and
 609 J.-H. Yee (2002), High Resolution Doppler Imager observations of ozone in
 610 the mesosphere and lower thermosphere, *J. Geophys. Res.*, *107*, 4390, doi:
 611 10.1029/2001JD001505.
- 612 Marsh, D. R., R. R. Garcia, D. E. Kinnison, B. A. Boville, F. Sassi, S. C. Solomon,
 613 and K. Matthes (2007), Modelling the whole atmosphere response to solar cycle
 614 changes in radiative and geomagnetic forcing, *J. Geophys. Res.*, *112*(D23306),
 615 doi:10.1029/2006JD008306.
- 616 Mlynczak, M. G., B. T. Marshall, F. J. Martin-Torres, J. M. Russel III, R. E.
 617 Thompson, E. E. Remsberg, and L. L. Gordley (2007), Sounding of the Atmo-
 618 sphere using Broadband Emission Radiometry observations of daytime meso-
 619 spheric O₂(¹ Δ) 1.27 μ m emission and derivation of ozone, atomic oxygen, and
 620 solar and chemical energy deposition rates, *J. Geophys. Res.*, *112*, D15,306, doi:
 621 10.1029/2006JD008355.
- 622 Moran, T., P. Foukal, and D. Rabin (1992), A photometric study of faculae and
 623 sunspots between 1.2 and 1.6 micron, *Sol. Phys.*, *142*, 35–46.
- 624 Neckel, H., and D. Labs (1984), The solar radiation between 3300 and 12500Å, *Sol.*
 625 *Phys.*, *90*, 205–258.
- 626 Oberländer, S., U. Langematz, K. Matthes, M. Kunze, A. Kubin, J. Harder, N. A.
 627 Krivova, S. K. Solanki, J. Pagaran, and M. Weber (2012), The influence of spec-
 628 tral solar irradiance data on stratospheric heating rates during the 11 year solar
 629 cycle, *Geophys. Res. Lett.*, *39*, L01,801, doi:10.1029/2011GL049539.
- 630 Pagaran, J., M. Weber, and J. P. Burrows (2009), Solar variability from 240 to 1750
 631 nm in terms of faculae brightening and sunspot darkening from SCIAMACHY,
 632 *Astron. J.*, *700*, 1884–1895.
- 633 Pagaran, J., G. Harder, M. Weber, L. Floyd, and J. P. Burrows (2011a), Intercom-
 634 parison of SCIAMACHY and SIM vis-IR irradiance over several solar rotational
 635 timescales, *Astron. Astrophys.*, *528*, A67, doi:10.1051/0004-6361/201015632.
- 636 Pagaran, J., M. Weber, M. DeLand, L. Floyd, and J. P. Burrows (2011b), Solar spec-
 637 tral irradiance variations in 240-1600 nm during the recent solar cycles 21-23,
 638 *Sol. Phys.*, *XX*, XX–XX.
- 639 Remsberg, E. E. (2008), On the response of Halogen Occultation Experiment
 640 (HALOE) stratospheric ozone and temperature to the 11-year solar cycle forc-
 641 ing, *J. Geophys. Res.*, *113*(D22304), doi:10.1029/2008JD010189.
- 642 Remsberg, E. E., B. T. Marshall, M. Garcia-Comas, D. Krueger, G. S. Lingen-
 643 felser, J. Martin-Torres, M. G. Mlynczak, J. M. Russel III, A. K. Smith, Y. Zhao,
 644 C. Brown, L. L. Gordley, M. J. Lopez-Gonzales, M. Lopez-Puertas, C.-Y. She,
 645 M. J. Taylor, and R. E. Thompson (2008), Assesment of the quality of the Ver-
 646 sion 1.07 temperature-versus-pressure profiles of the middle atmosphere from
 647 TIMED/SABER, *J. Geophys. Res.*, *113*, D17,101, doi:10.1029/2008JD010013.
- 648 Rohen, G., C. von Savigny, M. Sinnhuber, E. J. Llewellyn, J. W. Kaiser, C. H.
 649 Jackman, M.-B. Kallenrode, J. Schröter, K.-U. Eichmann, H. Bovensmann, and

- 650 J. P. Burrows (2005), Ozone depletion during the solar proton events of Octo-
651 ber/November 2003 as seen by SCIAMACHY, *J. Geophys. Res.*, *110*, A09S39,
652 doi:10.1029/2004JA010984.
- 653 Rong, P. P., J. M. Russell III, M. G. Mlynczak, E. E. Remsberg, B. T. Marshall,
654 L. L. Gordley, and M. Lopez-Puertas (2008), Validation of TIMED/SABER v1.07
655 ozone at 9.6 μm in the altitude range 15–70 km, *J. Geophys. Res.*, *114*, D04,306,
656 doi:10.1029/2008JD010073.
- 657 Rottman, G., L. Floyd, and R. Viereck (2004), Measurement of solar ultraviolet
658 irradiance, *Geophys. Mono.*, *41*, 111–125, doi:10.1029/141GM10.
- 659 Russell III, J. M., M. G. Mlynczak, L. L. Gordley, J. J. Tansock Jr., and R. W. Esplin
660 (1999), Overview of the SABER experiment and preliminary calibration results,
661 *Proc. SPIE*, *3756*(277), doi:10.1117/12.366382.
- 662 Schmidt, H., G. P. Brasseur, M. Charron, E. Manzini, M. A. Giorgetta, T. Diehl,
663 V. I. Fomichev, D. Kinnison, D. Marsh, and S. Walters (2006), The HAMMONIA
664 Chemistry climate model: Sensitivity of the mesopause region to the 11-year solar
665 cycle and CO₂ doubling, *J. Climate*, *19*, 3903–3931.
- 666 Sekiyama, T. T., K. Shibata, M. Deushi, K. Kodera, and J. L. Lean (2006), Strato-
667 spheric ozone variation induced by the 11-year solar cycle: Recent 22-year sim-
668 ulation using 3-D chemical transport model with reanalysis data, *Geophys. Res.
669 Lett.*, *33*(L17812), doi:10.1029/2006GL026711.
- 670 Skupin, J., S. Noël, M. W. Wuttke, M. Gottwald, H. Bovensmann, M. We-
671 ber, and J. P. Burrows (2005a), SCIAMACHY solar irradiance observation in
672 the spectral range from 240 to 2380 nm, *Adv. Space Res.*, *35*, 370–375, doi:
673 10.1016/j.asr.2005.03.036.
- 674 Skupin, J., M. Weber, S. Noël, H. Bovensmann, and J. P. Burrows (2005b), GOME
675 and SCIAMACHY solar measurements: Solar spectral irradiance and Mg II solar
676 activity proxy indicator, *Mem. Soc. Astron. Ital.*, *76*, 1038–1041.
- 677 Solomon, S. C., L. Qian, L. V. Didkovsky, R. A. Viereck, and T. N. Woods (2011),
678 Causes of low thermospheric density during the 2007–2009 solar minimum, *J.
679 Geophys. Res.*, *116*, doi:10.1029/2011JA016508, in press.
- 680 Sonkaew, T., V. V. Rozanov, C. von Savigny, A. Rozanov, H. Bovensmann, and
681 J. P. Burrows (2009), Cloud sensitivity studies for stratospheric and lower meso-
682 spheric ozone profile retrievals from measurements of limb scattered solar radia-
683 tion, *Atmos. Meas. Tech.*, *2*, 653–678, doi:10.5194/amt-2-653-2009.
- 684 Thuillier, G., L. Floyd, T. N. Woods, R. Cebula, E. Hilsenrath, M. Hersé, and
685 D. Labs (2004), Solar irradiance reference spectra, in *Solar Variability and its
686 Effects on Climate. Geophysical Monograph 141*, vol. 141, edited by J. M. Pap,
687 P. Fox, C. Fröhlich, J. K. H. S. Hudson, J. McCormack, G. North, W. Sprigg, and
688 S. T. Wu, pp. 171–194.
- 689 Unruh, Y. C., N. A. Krivova, S. K. Solanki, J. W. Harder, and G. Kopp (2008),
690 Spectral irradiance variations: comparison between observations and the SATIRE
691 model on solar rotation time scales, *Astron. Astrophys.*, *486*, 311–323, doi:
692 10.1051/0004-6361:20078421.

- 693 Viereck, R. A., and L. C. Puga (1999), The NOAA Mg II core-to-wing solar index:
694 Construction of a 20-year times series of chromospheric variability from multiple
695 satellites, *J. Geophys. Res.*, **104**, 9,995–10,005.
- 696 Viereck, R. A., L. Puga, D. McMullin, D. Judge, M. Weber, and W. K. Tobiska
697 (2001), The Mg II index: A proxy for solar EUV, *Geophys. Res. Lett.*, **28**, 1343–
698 1346.
- 699 Viereck, R. A., L. E. Floyd, P. C. Crane, T. Woods, B. G. Knapp, G. Rottman,
700 M. Weber, L. C. Puga, and M. T. DeLand (2004), A composite Mg II index span-
701 ning from 1978 to 2003, *Space Weather*, **2**, S10,005.
- 702 von Savigny, C., A. Rozanov, H. Bovensmann, K.-U. Eichmann, S. Noël, V. V.
703 Rozanov, M. Weber, J. P. Burrows, and J. W. Kaiser (2005), The ozone hole
704 breakup in September 2002 as seen by SCIAMACHY on ENVISAT, *J. Atmos.
705 Sci.*, **62**, 721–734.
- 706 Weber, M. (1999), Solar Activity during solar cycle 23 monitored by GOME,
707 in *ESA-WPP 1999: European Symposium on Atmospheric Measurements from
708 Space, Proc. ESAMS '99, ESA Special Publication*, vol. 161, pp. 611–616, ESA
709 Publications Division, Nordwijk.
- 710 Weber, M., J. P. Burrows, and R. P. Cebula (1998), GOME solar uv/vis irradiance
711 measurements between 1995 and 1997 - First results on proxy solar activity stud-
712 ies, *Sol. Phys.*, **177**, 63–77.
- 713 Wehrli, C. (1985), Extraterrestrial solar spectrum, *Tech. rep.*, Physikalisch-
714 Meteorologisches Observatorium, World Radiation Center (PMO/WRC), Publi-
715 cation No. 615.